J Mater Sci: Mater Med (2006) 17:989–996
DOI 10.1007/s10856-006-0434-x

Controlling ion release from bioactive glass foam scaffolds with antibacterial properties

Julian R. Jones · Lisa M. Ehrenfried · Priya Saravanapavan · Larry L. Hench

Received: 24 January 2006 / Accepted: 10 February 2006

Abstract Bioactive glass scaffolds have been produced, which meet many of the criteria for an ideal scaffold for bone tissue engineering applications, by foaming sol-gel derived bioactive glasses. The scaffolds have a hierarchical pore structure that is very similar to that of cancellous bone. The degradation products of bioactive glasses have been found to stimulate the genes in osteoblasts. This effect has been found to be dose dependent. The addition of silver ions to bioactive glasses has also been investigated to produce glasses with bactericidal properties. This paper discusses how changes in the hierarchical pore structure affect the dissolution of the glass and therefore its bioactivity and rate of ion delivery and demonstrates that silver containing bioactive glass foam scaffolds can be synthesised. It was found that the rate of release of Si and Ca ions was more rapid for pore structures with a larger modal pore diameter, although the effect of tailoring the textural porosity on the rate of ion release was more pronounced. Bioactive glass scaffolds, containing 2 mol% silver, released silver ions at a rate that was similar to that which has previously been found to be bactericidal but not high enough to be cytotoxic to bone cells.

1 Introduction

Bone tissue engineering is one form of regenerative medicine that may help the body's own regenerative mechanisms to restore a diseased or damaged tissue to its original state and function, reducing the need for transplants and joint replacements [1–3]. An ideal strategy for the tissue engineering of bone is the harvesting of osteogenic cells from the patient, which are expanded in culture and seeded on a scaffold that acts as guide and stimulus for tissue growth in three dimensions [4, 5]. The osteogenic cells lay down bone extracellular matrix in the shape of the scaffold as woven (immature) bone. The tissue engineered construct (or biocomposite) can then be implanted into the patient and eventually the synthetic scaffold should resorb as the bone is remodelled into mature bone.

1.1 An ideal scaffold

The general criteria for an ideal scaffold for bone tissue engineering are listed elsewhere [6], but the scaffold must stimulate cells to lay down bone in three dimensions (3D). To do this, it must have an open porous structure to allow cell penetration, tissue ingrowth and eventually vascularisation on implantation. The minimum aperture diameter for *in vivo* bone ingrowth has been much debated but is thought to be 100 μm. The criteria for an optimised pore network for *in vitro* bone growth are less clear, especially if the scaffold resorbs *in vitro* and the structure changes before implantation.

During implantation of a tissue engineering construct there is a risk of infection. Sterilisation of a tissue/scaffold biocomposite is difficult as tissue is involved. The procedure would be to use a sterile scaffold and grow tissue in a sterile environment prior to implantation. Therefore it would be advantageous if the scaffold would deliver antibacterial agents to the implant site after implantation.

Bioactive materials have the potential to be used in scaffolds as they stimulate new bone growth and bond to bone [1]. Bioactive glasses are one example.

J. R. Jones (✉) · P. Saravanapavan · L. L. Hench
Department of Materials, Imperial College London, South Kensington Campus, London SW7 2AZ
e-mail: julian.r.jones@imperial.ac.uk

L. M. Ehrenfried
Cambridge Centre for Medical Materials, Department of Materials Science and Metallurgy, University of Cambridge, Pembroke Street, Cambridge CB2 3QZ, U.K.

1.2 Bioactive glasses

The mechanism of bone bonding to bioactive glasses is the formation of a carbonate substituted hydroxycarbonate apatite layer (HCA) on the surface of the materials after immersion in body fluid. This layer is similar to the apatite in bone and therefore a strong bond can form [7]. Bioactive glasses are osteoproductive, which means they stimulate new bone growth on their surface, even away from the glass/bone interface [1]. Importantly for bone regeneration, bioactive glasses are resorbable and the dissolution products (soluble silicon and calcium) have been found to up-regulate seven families of genes in osteoblasts [8]. It was found that both Ca and Si ions had to be present for the up-regulation to occur and the effect was found to be dose-dependant. It is therefore vital that the ion release from any bioactive scaffold can be tailored.

There are two types of bioactive glasses; melt-derived and sol-gel derived. The original bioactive glass discovered by Hench and named Bioglass® is a melt-derived glass with four components (46.1% SiO_2, 24.4% Na_2O, 26.9% CaO and 2.6% P_2O_5, in mol) [9, 10]. Pores have been introduced into melt-derived bioactive glasses but the pores were few in number and were in the form of orientated channels of irregular diameter running through the glass so interconnectivity was poor [11].

1.3 Sol-gel derived bioactive glasses

Sol-gel derived bioactive glasses were developed by Hench and co-workers at the University of Florida in the early 1990s [12–15] and became the focus for Hench's team Imperial College when he moved there in 1995 [16–18], along with his work on gene stimulation. Sol-gel derived bioactive glasses are synthesised by the hydrolysis of alkoxide precursors to form a sol, which is a colloidal silica solution. The sol then undergoes polycondensation to form a silica network (gel). The gel is then heat treated to form a glass [12]. A liquor of water and alcohol is a byproduct of condensation and is trapped in the silica network. During drying the liquid evaporates leaving a nanometer scale pore network, which causes sol-gel derived bioactive glasses to be more bioactive and to resorb quicker than melt-derived glasses of similar compositions [19]. The pore structure increases the specific surface area by two orders of magnitude compared to a melt-derived glass of a similar composition [19].

The 58S composition (60 mol% SiO_2, 36 mol% CaO and 4 mol% P_2O_5) compositions was the focus of the early work [13–15] and a binary composition (70 mol% SiO_2, 30 mol% CaO) was developed by Saravanapavan et al. [17] at Imperial College London, which was also found to be bioactive.

1.4 Antibacterial properties

For many implants, a sustained and controlled relasese of antibacterial agents into the wound site is desirable to combat infection. A further advantage of sol-gel derived glasses is that silver, which is known to have antibacterial properties, can be incorporated into glass compositon [20, 21]. Bellantone et al. [20, 21] compared the *in vitro* antibacterial action of silver doped, in the system SiO_2-CaO-P_2O_5-Ag_2O, with those of its SiO_2-CaO-P_2O_5 (58S) counterpart. The incorporation of 3-wt% Ag_2O in the glass provided antimicrobial properties without compromising its bioactivity. The silver doped glass exhibited a marked bactericidal effect on *E. coli* MG1655, *Pseudomonas aeruginosa*, and *Staphylococcus aureus* with a minimum inhibiting concentration of 0.2 mg (biomaterial)/mL (culture solution), above which bacterial growth was reduced to 0.01% of that of the control culture. A complete bactericidal effect was elicited within the first hours of incubation at silver-doped bioactive glass concentrations of 10 $mgml^{-1}$. In comparison, neither the equivalent 3 component sol-gel derived bioactive glass nor the melt-dervied 45S5 Bioglass® possessed antimicrobial properties over the concentration range investigated (0.1–40.0 mg/ml).

1.5 Bioactive glass scaffolds

By foaming sol-gel derived bioactive glasses, we have previously produced scaffolds with a hierarchical pore structure similar to trabecular bone [22]. As the foam is made from sol-gel derived bioactive glass, the 3D interconnected solid network has a textural porosity with diameters in the range 2–20 nm, termed mesoporosity. Tertiary (SiO_2, CaO, P_2O_5), binary (SiO_2, CaO) and unary systems (SiO_2) were all be successfully foamed as scaffolds [22]. Scaffolds of the 58S composition have been found to cause primary human osteoblasts to lay down bone extracellular matrix (mainly collagen type I), which mineralised after 10 days of culture without the addition of dexamethasone and β-glycerophosphate [23].

It is important to be able to tailor the structure of the scaffolds. Previously, we have found that variables in each stage of the foaming process (Fig. 1) have an effect on the pore structure. Such variables include the sol (glass) composition and surfactant concentration [24], gelling agent concentration, the temperature at which the process is carried out and whether additional water is added with the surfactant to improve its efficiency [25]. The glass composition was conducive to foaming was the 70S30C composition and the most efficient method to control the aperture diameter was to change the surfactant concentration [6]. The most efficient method of changing the nanoscale textural porosity was

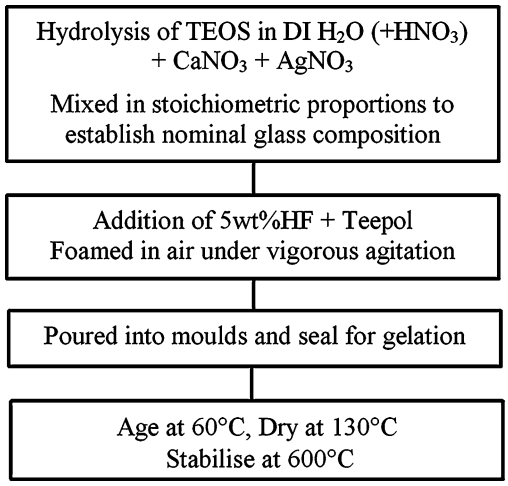

Fig. 1 A flow diagram of the process for producing bioactive glass foam scaffolds

found to be sintering the scaffolds to different temperatures [27]. By sintering 70S30C scaffolds with a bulk density (ρ_b) of 0.25 gcm^{-3}, a modal interconnected pore diameter (D_{mode}) of 140 μm and a modal textural pore diameter (d_{mode}) of 17 nm at 800°C for 2 h, ρ_b increased, due to a densification of the foam struts as the d_{mode} decreased to 12 nm. This caused the maximum compressive strength of the scaffolds to increase from 0.25 MPa to 2.36 MPa [27], which is similar to that of porous synthetic hydroxyapatite implants [27]. Importantly, the D_{mode} was 98 μm, which is thought to be suitable for bone tissue engineering. X-ray diffraction spectra confirmed that the scaffolds were amorphous after sintering at 800°C. From this previous work, sintering at 800°C for 2 h was thought to be an optimal condition for scaffold production. An aim of this work is to investigate how changing the ρ_b, by using different surfactant concentrations, affects the dissolution rate of the scaffolds that are sintered at 800°C.

This paper discusses the effect of changes in the pore network and the final sintering temperature on ion release and bioactivity and shows how antibacterial agents can be introduced into the scaffold composition and how the bioactivity and release of the gene stimulating and antibacterial ions can be controlled by tailoring processing conditions.

2 Materials and methods

2.1 Synthesis

Figure 1 shows a flow chart of the sol-gel foaming process. A sol of the 70S30C (70 mol% SiO_2, 30 mol% CaO) composition was synthesised by the hydrolysis of TEOS (tetraethyloxysilane), using a water: TEOS molar ratio (R ratio) of 12. Calcium was introduced into the composition by adding calcium nitrate tetrahydrate. Unless otherwise stated, all reagents were from Sigma, Dorset. After hydrolysis is completed, aliquots of 50 ml of sol were foamed by vigorous agitation in air while a gelling agent (hydrofloric acid, HF) was added to rapidly increase the viscosity of the sol. A surfactant was also added to lower the surface tension and stabilise the air bubbles. The bubbles were permanently stabilised by the final gelation reaction (polycondensation). The surfactant used was Teepol (Thames Mead, London), which is a mixture of ionic (<15vol%) and non-ionic (<5vol%) surfactants. In order to obtain scaffolds with 3 different interconnected pore size distributions, 50 ml of sol of were foamed with surfactant volumes of 0.30, 0.35 and 0.38 ml of Teepol. The gelled foams were aged at 60°C, dried at 130°C and stabilised at 600°C, using carefully controlled heating rates (1°C/min).

The scaffolds were then sintered at 800°C for 2 h to increase the density of the foam struts and to improve mechanical properties.

Antibacterial foams of a similar composition (70 mol% SiO_2, 29 mol% CaO, 1 mol% Ag_2O) were produced by substituting Ag for Ca using silver nitrate as a precursor for Ag_2O. Their final sintering temperature was 600°C. Foams were produced and stored in a darkened room to prevent light catalysed oxidation of the silver ion.

2.2 Characterisation

The geometrical bulk densities of the foam scaffolds were calculated from dimensional and mass measurements.

The foams were characterised using a scanning electron microscopy (JEOL 5610LV) with 5 kV accelerating voltage and mercury intrusion porosimetry (PoreMaster 33, Quantachrome) to measure interconnected macropore size distributions. Mercury porosimetry only measures pores that are interconnected, therefore the mode of the interconnected macropore distributions was used as a guide to the aperture diameter distribution of the foams. X-ray micro-computed tomography (XMT) image of the scaffolds were obtained using a commercial XMT unit (Phoenix X-ray Systems and Services GmbH).

Textural pore size distributions were derived using the BJH method on isotherms obtained from nitrogen sorption analysis (Autosorb AS6, QuantaChrome) [16].

2.3 Dissolution and bioactivity tests

A previous study found there to be a dose-dependent effect on not only the rate of HCA layer formation on bioactive glasses but on whether a layer forms at all [28]. Under high concentrations of glass in simulated body fluid (SBF), calcite can form at the expense of HCA. Therefore 0.075 g of foam was immersed in 50ml of SBF and placed in an orbital shaker

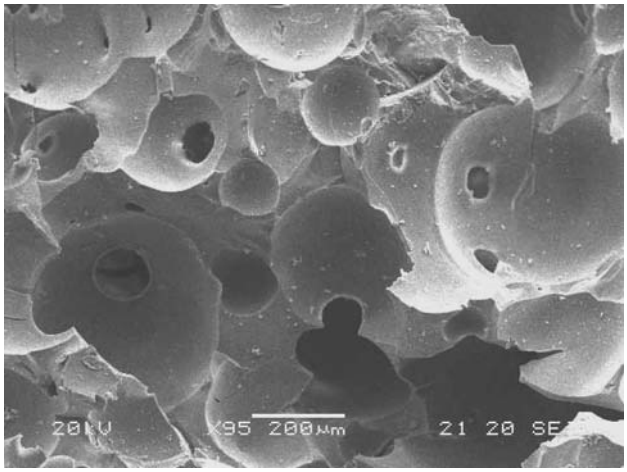

Fig. 2 SEM image of a bioactive glass scaffold foamed with 0.35 ml Teepol and sintered at 800°C

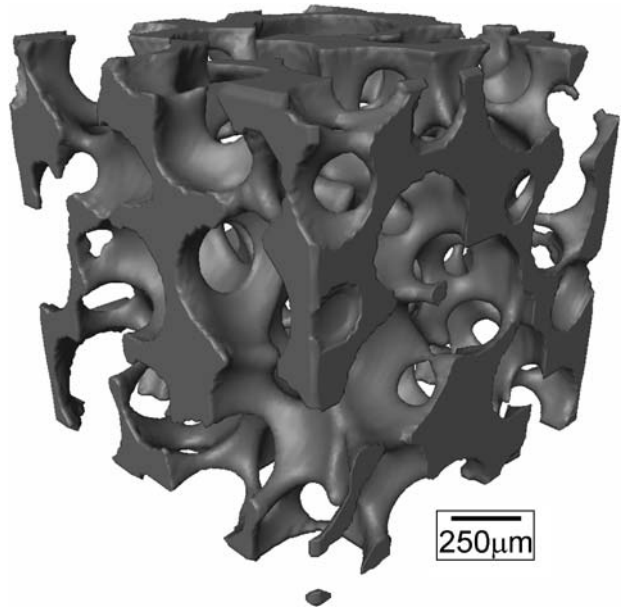

Fig. 3 XMT image of a bioactive glass foam scaffold foamed with 0.35 ml Teepol and sintered at 800°C

at 37°C, for 1 h, 2 h, 4 h, 24 h and 72 h, 172 h at an agitation rate of 175 Hz. Three samples were run per time point, with the average values reported.

Extracts obtained by filtration were analysed by ICP (Inductive Coupled Plasma Spectroscopy, Thermo FI ARL 3580 B) for Si, Ca, P and Ag concentration in solution. The filtrated foam was washed with acetone to terminate the reaction, dried and then evaluated by X-ray diffraction (XRD) and Fourier transform infrared (FTIR) spectroscopy. Absorbance FTIR spectra were collected using a Mattson Genesis II spectrometer, with a Pike Technologies EasiDiff diffuse reflectance accessory in the range 400–1600 cm^{-1}.

2.4 Compression testing

Parallel plate compression tests were carried out on cylindrical foams, with heights of 9 mm and diameters of 27 mm using an Instron with a crosshead velocity of 0.5 mm/min and a 1 kN load cell.

3 Results and discussion

3.1 Pore morphologies

Figure 2 shows a scanning electron micrograph (SEM) of a bioactive glass foam of the 70S30C composition foamed with 0.35 ml of Teepol and sintered at 800°C for 2 h. Figure 2 shows that the foam is comprised of large macropores with diameters in the region of 200–600 μm that are highly interconnected. Many of the interconnect apertures (dark areas) have diameters in excess of the 100 μm required for tissue engineering applications.

SEM micrographs can be misleading however. SEM micrographs are images of fracture surfaces; therefore the real 3D shape and connectivity of the pores cannot be seen or quantified. It is vital to be able to obtain a 3D pore size distribution of tissue scaffolds by non-destructive means [26]. Figure 3 shows an XMT image of a similar scaffold, to that shown in Fig. 2. Figure 3 shows that the macropore network is very highly interconnected and is very similar to that of trabecular bone found in the literature [29]. The pore shape and size is homogeneous because the pores form in a liquid that is well agitated with the surfactant well dispersed. Connectivity occurs because the spherical air bubbles are all in contact with each other immediately prior to gelation, separated only by a thin film of silica-based sol that is stabilised by the surfactant. Upon gelation and subsequent thermal processes the thin film drains, shrinkage occurs and the surfactant is combusted, leaving the apertures. The scaffolds have interconnected macropores that have the potential to allow cell migration into the scaffold and stimulate growth of new tissue in 3D.

3.2 Pore network characterisation

From helium pycnometry, the true density of all the foams sintered at 600°C was 2.8 gcm^{-3}. Following sintering at 600°C, the 3 Teepol concentrations provided ρ_b values of, 0.15, 0.25, and 0.35 gcm^{-3}, corresponding to percentage porosities of 94%, 91% and 87%. After sintering at 800°C, the true density remained unchanged but the ρ_b values changed to 0.25, 0.33 and 0.52 gcm^{-3} respectively, producing porosities of 91%, 88% and 81%. However, for tissue

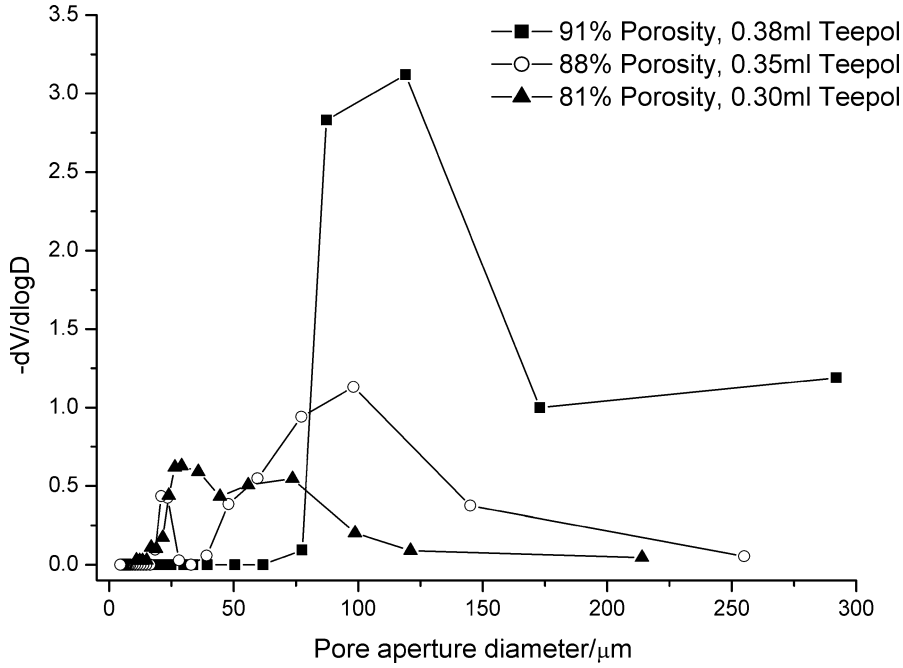

Fig. 4 Interconnected pore aperture distributions as a function of percentage porosity and the amount of Teepol used in foaming, obtained from mercury intrusion porosimetry

engineering applications, the percentage porosity is much less important than the interconnected pore diameters, as two scaffolds with the same percentage porosity can either be comprised of many small pores (suitable as a scaffold) or fewer large pores (more suitable).

The interconnected pore aperture distributions were obtained from mercury intrusion porosimetry (Fig. 4). Figure 4 shows that scaffolds that were foamed with 0.38 ml Teepol, had 91% porosity at 800°C and exhibited a modal interconnected pore diameter of 119.4 μm. When the surfactant content was reduced to 0.35 ml and 0.3 ml the modal pore diameter decreased to 98.1 μm and 73.6 μm respectively. 98.1 μm should be a suitable pore size for tissue engineering applications as there appears to be many apertures larger than the mode (Fig. 4). In constrast, the pore size distribution for scaffolds foamed with 0.3 ml Teepol was broad, bimodal and showed few pores above 100 μm. The lower mode of the distribution was 29 μm. The bimodal distribution was caused by there being insufficient surfactant to lower the surface tension of the sol to a level that would create a homogeneous distribution of pores. Scaffolds produced with these porosities are unlikely to be useful in tissue engineering applications.

Mercury intrusion porosimetry is a useful tool, however it is a destructive technique and it only measures a distribution of the apertures. A non-destructive technique is required that will quantify the full complex pore structure of tissue scaffolds. Many authors use 3D XMT images of porous scaffolds, however, for tissue scaffolds it is imperative to be able to quantify the sizes of the large pores and the apertures connecting the pores. We have been able to do this by using 3 computer algorithms, as described in detail in refs [6, 30]. The individual pores and apertures objects were quantified to obtain pore aperture and pore size distributions non-destructively. Scaffolds sintered at 800°C with a $\rho_b = 0.33\ \mathrm{gcm}^{-3}$ were found to have a broad modal interconnected pore diameter peak of 80–211 μm [6].

3.3 Ion release and bioactivity

Previous work has shown that when the final sintering temperature of a scaffold increased from 600°C to 800°C the dissolution rate decreased, which caused the rate of formation of the HCA layer to decrease [26]. For example, for foams produced with 0.35 ml Teepol and sintered at 600°C with percentage porosity of 94%, 125 $\mu\mathrm{gml}^{-1}$ of Si was released after 24 h of immersion. For the same foams sintered at 800°C (reduced to 88% porosity after sintering) the release of Si was 65 $\mu\mathrm{gml}^{-1}$. The HCA layer formed after 8 h on scaffolds sintered at 600°C, but it took 3 days to form on scaffolds sintered at 800°C. This work shows that changes in the pore network, by controlling the surfactant concentration during foaming, affected the dissolution process. Figure 5 shows the dissolution profiles (in SBF) of silicon, calcium and phosphate ions of foams produced with 0.30, 0.35 and 0.38 ml of surfactant and corresponding percentage porosities of 91%, 88% and 81% respectively, sintered at 800°C. Figures 6 and 7 show FTIR spectra of scaffolds sintered at 800°C, with 91% porosity (95% porosity prior to sintering) and 88% porosity (94% porosity prior to sintering) respectively, following immersion in SBF as a function of time. Figure 5 shows that the release of the gene activating Si species was 65 $\mu\mathrm{gml}^{-1}$

Table 1 Characterisation summary of foams sintered at 800°C

ρ_b = bulk density ρ_r = relative density, D = interconnected pore window diameter from mercury porosimetry.

Teepol (ml)	ρ_b (gcm^{-1})	ρ_r (gcm^{-1})	% porosity	Modal D (μm)	t_{HCA} (h)	Compressive Strength MPa
0.38	0.26	0.09	91	119.4	24	1.6
0.35	0.33	0.12	88	98.1	72	2.3
0.30	0.52	0.19	81	73.6	72	2.5

after 24 h immersion for the scaffolds produced with percentage porosities of 88% and 81% and the dissolution profiles for Si, Ca and P were similar. The amount of phosphate in solution decreased because of the formation of a calcium phosphate (HCA) layer on the surface of the glass.

For these foams, the HCA layer formed within 3 days immersion (Fig. 7). As the percentage porosity increased to 91%, the Si release at 24 h increased to 107 μgml^{-1} and the Ca release increased by approximately 20%. The HCA layer formed after 24 h (Fig. 6). This is due to the strut size decreasing and the pore structure being more open (Fig. 4) allowing more rapid ion exchange, which is the first stage of the dissolution/bioactivity mechanism. The morphology of a potential scaffold will therefore have a large effect on rate of delivery and concentration of gene stimulating ions and therefore rate of bone bonding and regeneration of bone.

3.4 Mechanical properties

Table 1 shows a summary of the effects of percentage porosity on the properties. Table 1 shows that the compressive strength increased as percentage porosity decreased due to density of the scaffolds increasing. The highest strength (2.51 MPa) was obtained for scaffolds that were found to have a heterogeneous pore network, using 0.3 ml Teepol. A scaffold with 88% porosity (0.35 ml Teepol) had a compressive strength of 2.3 MPa. When more Teepol was used (0.38 ml), the modal interconnected pore diameter was increased to 119 μm, but the compressive strength was reduced to 1.6 MPa. In previous work, scaffolds sintered at 600°C, with 94% porosity and with an interconnected pore diameter of 122 μm, exhibited a compressive strength of 0.26 MPa, which is an order of magnitude lower [26]. The higher sintering temperature is therefore beneficial and a balance must therefore be drawn between strength, the interconnectivity of the pore network and ion release.

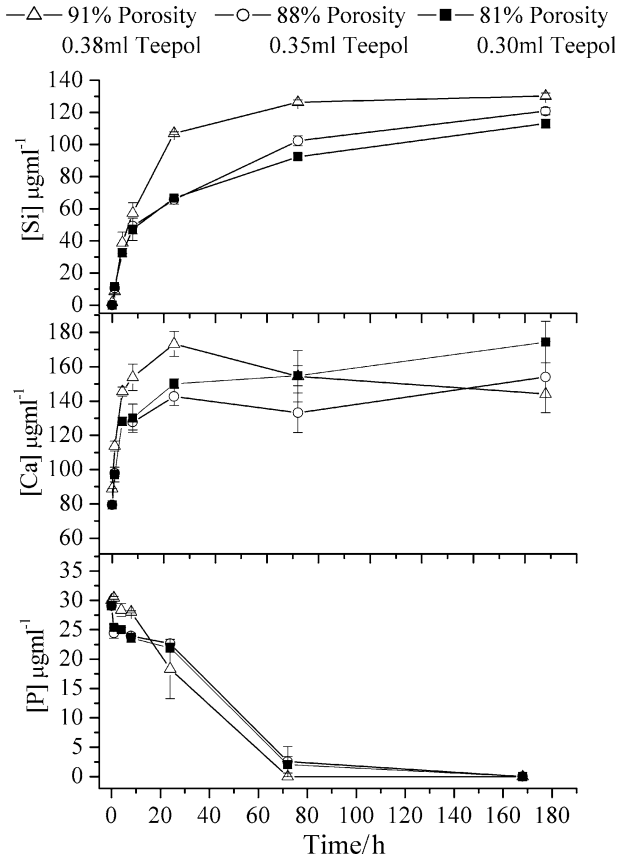

Fig. 5 Dissolution profiles (from ICP) of foams as a function of percentage porosity and immersion time in SBF at 37°C under 175 rpm

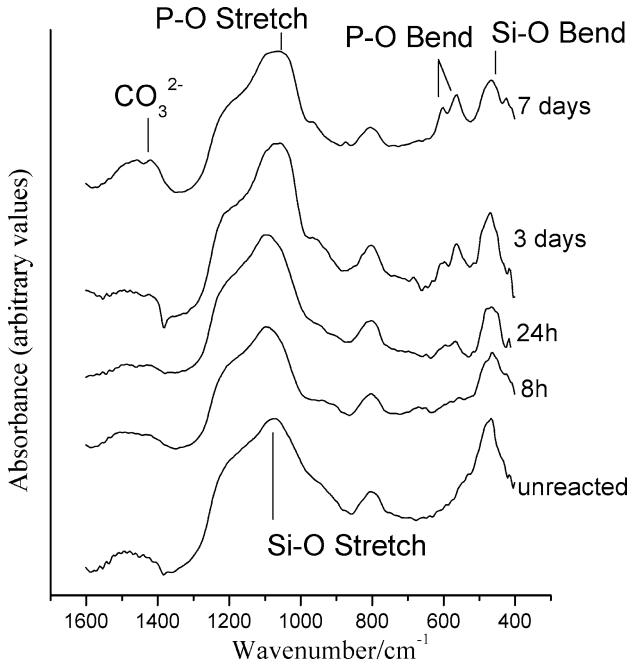

Fig. 6 FTIR spectra of scaffolds sintered at 800°C, with 91% porosity (95% porosity prior to sintering)

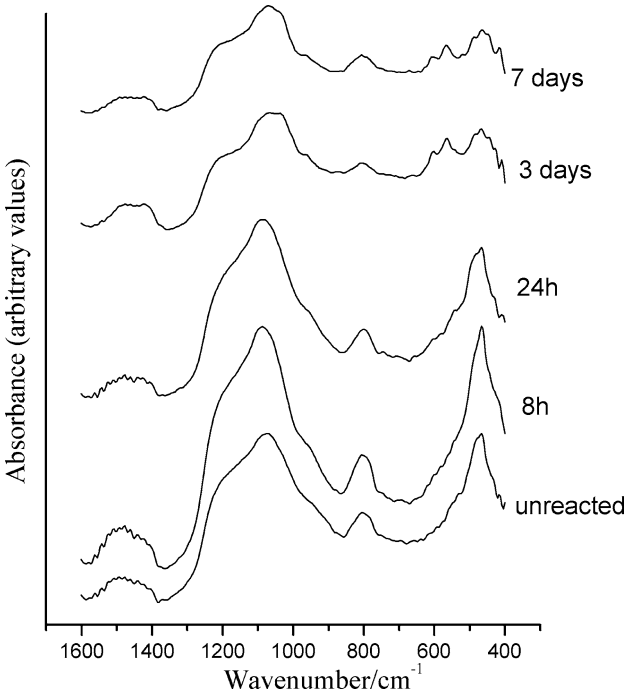

Fig. 7 FTIR spectra of scaffolds sintered at 800°C, with 88% porosity (94% porosity prior to sintering)

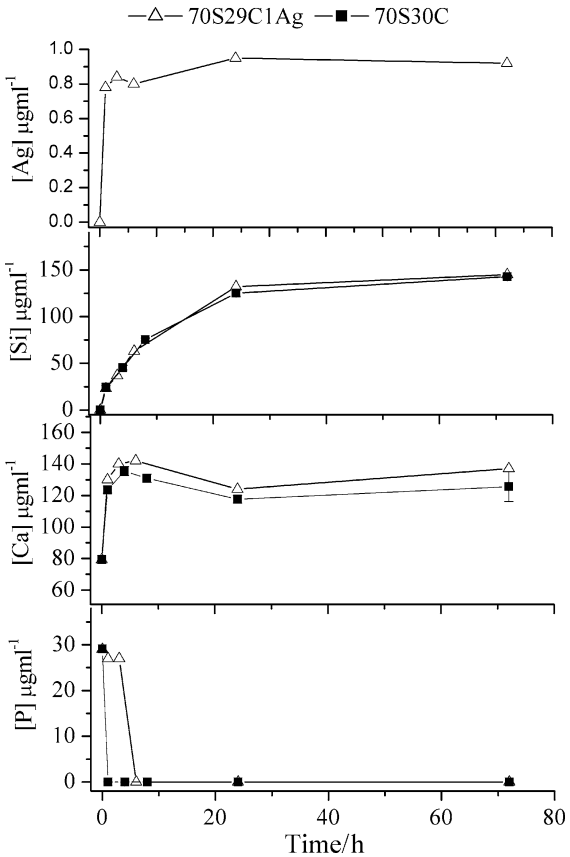

Fig. 8 Dissolution profiles (from ICP) of foams with and without silver in their compositions, as a function of immersion time in SBF at 37°C under 175 rpm

3.5 Antibacterial ion release

Foam scaffolds containing silver were successfully produced. Figure 8 shows the Ag, Si, Ca and P content of SBF as a function of immersion time for scaffolds of the 70S30C and 70S29C1Ag composition, obtained from ICP, following immersion in SBF. The scaffolds had 94% porosity and modal interconnected pore diameters between 120 and 140 μm. Figure 8 shows that the Si and Ca release profiles were unsurprisingly similar, due to the small amounts of Ag that would be substituting into the glass. Ag would be present as a network modifier, therefore it is not tightly bound into the network and would be expected to leave the glass during the cation exchange part of the glass dissolution mechanism.

Figure 8 shows that this is the case as 0.75 μgml^{-1} of Ag was released within the first hour of immersion. However, during the next 23 h the release was slower and reached 0.95 μgml^{-1}. The latter value has been found to have a bactericidal effect on E. coli, P. aeruginosa and S. aureus cultures [21]. The amount of silver release from the silver-doped foams was above the minimum required to have a bactericidal effect in culture (0.1 μgml^{-1}) and it was also below the cytotoxic concentration (1.6 μgml^{-1}) for somatic cells [21]. Sintering the scaffolds to higher temperatures, such as 800°C, may allow a prolonged and more easily controlled rate of Ag release.

From the P dissolution profile, the formation of the HCA layer appears to be delayed compared to the silver free composition. However, the HCA layer was detected after 6 h of immersion in SBF by FTIR (not shown), therefore the presence of silver in the bioactive gel-glass foams did not adversely affect the bioactivity. In fact it has been suggested that silver ions in the glass surface cause preferential binding of phosphate ions in the formation of nanoclusters of silver phosphate, which may act as nucleation sites for the formation of HCA. The release of Ag ions into SBF may also reduce the minimum ion product of calcium and phosphate necessary for the precipitation of HCA [31].

In order to develop a scaffold for direct implantation into load bearing sites, bioactive inorganic/organic hybrid scaffolds should be developed, using biodegradable polymers [32]. This process will also affect the ion release properties and the cell response.

4 Conclusions

The pore network of bioactive glass scaffolds can be controlled by varying the surfactant concentration used in the foaming process, however below 0.3 ml of Teepol per 50 ml of sol the pore network becomes heterogeneous.

Sol foamed using 0.35 ml of Teepol, produced scaffolds with 94% porosity and a modal interconnected pore diameter of 122 μm with a sintering temperature of 600°C. These

scaffolds were sintered at 800°C for 2 h to improve mechanical properties and reduce the ion release to levels more suitable for cell stimulation, while maintaining a modal interconnected pore diameter (98 μm) suitable for tissue engineering applications. A compressive strength of 2.3 MPa was achieved. When more Teepol was used (0.38 ml), the modal interconnected pore diameter was increased to 119 μm, but the compressive strength was reduced to 1.6 MPa. This is still an order of magnitude higher than that for scaffolds sintered at 600°C with similar modal interconnected pore diameters.

The composition of bioactive glass sol-gel derived foam scaffolds can be modified to contain silver, which is known to have antibacterial properties, without compromising its bioactivity.

The sol-gel foaming process is a technique that can be used to produce bioactive glass scaffolds with spherical interconnected pores and tailored ion release and mechanical properties.

Acknowledgments The authors thank the Royal Academy of Engineering, the EPSRC and the Lloyds Tercetenary Foundation for financial support.

References

1. L. L. HENCH and J. M. POLAK, *Science* **295** (2002) 1014.
2. J. E. DAVIES, "Bone Engineering", (EM^2 incorporated, Toronto, 2000).
3. R. LANGER and J. P. VACANTI, *Science* **260** (1993) 920.
4. H. OHGUSHI and A. I. CAPLAN, *J. Biomed. Mater. Res. B.* **48** (1999) 913.
5. T. TAKEZAWA, *Biomaterials* **24** (2003) 2267.
6. J. R. JONES, P. D. LEE and L. L. HENCH, *Phil. Trans. R. Soc. A* **364** (2006) 263.
7. L. L. HENCH, *J. Am. Ceram. Soc.* **74** (1991) 1487.
8. I. D. XYNOS, A. J. EDGAR, L. D. K. BUTTERY, L. L. HENCH and J. M. POLAK, *J. Biomed. Mater. Res.* **155** (2000) 151.
9. L. L. HENCH, R. J. SPLINTER, W. C. ALLEN and T. K. GREENLEE, *J. Biomed. Mater. Res.* **2** (1971) 117.
10. L. L. HENCH, *J. Mat. Sci. Mater. Med*. This Issue
11. H. YUAN, J. D. DE BRUIJN, X. ZHANG, C. A. VAN BLITTERSWIJK and K. DE GROOT *J. Biomed*, *Mater. Res.* **58** (2001) 270.
12. L. L. HENCH and J. K. WEST, *Chem. Rev.* **90** (1990) 33.
13. L.L. HENCH and W. VASCONCELOS, *Ann. Rev. Mater. Sci.* 20 (1990) 269.
14. R. LI, A. E. CLARK and L. L. HENCH, *J. Appl. Biomat.* **2** (1991) 231.
15. M. M. PEREIRA, A. E. CLARK and L. L. HENCH *J. Biomed. Maters. Res.* **28** (1994) 693.
16. N. J. COLEMAN and L. L. HENCH, *Cer. Int.* **26** (2000) 171.
17. P. SARAVANAPAVAN, J. R. JONES, R. S. PRYCE and L. L. HENCH, *J. Biomed. Maters. Res.* **66A** (2003) 110.
18. J. R. JONES and L. L. HENCH, *J. Biomed. Maters. Res.* **68B** (2004) 36.
19. P. SEPULVEDA, J. R. JONES and L. L. HENCH *J. Biomed. Maters. Res.* **61** (2002) 301.
20. M. BELLANTONE, N. J. COLEMAN and L. L. HENCH, *J. Biomed. Mater. Res.* **51** (2000) 484.
21. M. BELLANTONE, H. D. WILLIAMS and L. L. HENCH, *Antim. Ag. Ch.* (2002) 1940.
22. P. SEPULVEDA, J. R. JONES and L. L. HENCH, *J. Biomed. Maters. Res.* **59** (2002) 340.
23. J. E. GOUGH, J. R. JONES and L. L. HENCH, *Biomaterials* **25** (2004) 2039.
24. J. R JONES and L. L. HENCH, *J. Mat. Sci.* **38** (2003) 3783.
25. J. R JONES and L. L. HENCH, *J. Biomed. Maters. Res.* **68B** (2004) 36.
26. J. R. JONES, L. M. EHRENFRIED and L. L. HENCH, *Biomaterials* **27** (2006) 964.
27. Implants for surgery–Hydroxyapatite–Part 1: Ceramic hydroxyapatite. BS ISO 13779-1:2000.
28. J. R. JONES, P. SEPULVEDA and L. L.HENCH. *J. Biomed. Mater. Res.* **58B** (2001) 720.
29. S. R. STOCK, *Int. Mat. Rev.* **44** (1999) 141.
30. R. ATWOOD, J. R. JONES, P. LEE and L. L. HENCH, *Scripta Mat.* **51** (2004) 1029.
31. M. SHIRKHANZADEH and M. AZADEGAN, *J. Mat. Sci.* **9** (1998) 385.
32. PEREIRA, J. R. JONES, R. L.OREFICE and L. L. HENCH, *J. Mat. Sci.: Mat. Med.* **16** (2005) 1045.